



Table 1: X-ray Data for the Three Complexes

	WT/2	Y216F/1	WT/1 <sup>a</sup>
<i>a</i> (Å)	98.6	99.8	99.3
<i>b</i> (Å)	51.0	51.7	51.4
<i>c</i> (Å)	51.2	51.7	51.2
<i>d</i> <sub>min</sub> (Å)	2.2	1.9	2.3
observations	34347	77769	83021
unique reflections	10991	15352	11014
% of possible	75	75	90
av <i>I</i> / $\sigma$ ( <i>I</i> )	8.8	14.2	14.1
<i>R</i> <sub>sym</sub> ( <i>I</i> ) <sup>b</sup>	0.067	0.053	0.057
highest shell, <i>d</i> (Å)	2.45	2.22	2.44
observations	8020	11695	14147
unique reflections	3959	5290	2843
% of possible	55	53	73
av <i>I</i> / $\sigma$ ( <i>I</i> )	1.6	4.4	6.8
<i>R</i> <sub>sym</sub> ( <i>I</i> ) <sup>b</sup>	0.38	0.20	0.22

<sup>a</sup> From Fan et al. (1994). <sup>b</sup> Weighted rms *R* factor on *I* (Howard et al., 1987). The space group for all complexes is *P*2<sub>1</sub>2<sub>1</sub>2.

ammonium sulfate in 25 mM MES buffer with 2 mM MgCl<sub>2</sub> and 2 mM NaN<sub>3</sub> at pH 6.5. Diamond-shaped crystals up to 0.55 mm × 0.3 mm × 0.1 mm grew at room temperature over a few weeks. The space group of the crystals is *P*2<sub>1</sub>2<sub>1</sub>2 with *Z* = 4, and cell dimensions are given in Table 1. These crystals are almost isomorphous with the complex containing D-Ala-D-Ala phosphinate **1** (Fan et al., 1994). Cocrystals with the D-Ala-D-lactate phosphonate could not be grown. The Y216F mutant DD-ligase (Shi & Walsh, 1995) was crystallized (without seeding with wild-type crystals) with 5 mM ATP and 5 mM **1** from 50% (v/v) saturated ammonium sulfate.

All diffraction data were collected at 22–23 °C on a Siemens area X-ray detector (512 × 512) with a Rigaku RU200 rotating anode X-ray generator operating at 38 kV and 180 mA with graphite-monochromatized Cu K $\alpha$  radiation. The  $\omega$  scan width was 0.2°, and the count time was 180 s per frame. Data reduction and scaling were done with XENGEN (Howard et al., 1987).

## RESULTS

**Refinement of the WT/2 Complex.** The initial protein model for the WT/2 complex was constructed from the coordinates of the WT/1 complex [Protein Data Bank entry 2DLN (Fan et al., 1994)]. The ligand-free model was refined with PROLSQ (Konnert & Hendrickson, 1980). Electron density mapping and fitting were carried out with CHAIN (Sack, 1988) and FRODO (Jones, 1985). When the standard *R* factor for the protein model reached 0.26, difference maps with coefficients  $|F_{o,complex}| - |F_{c,protein}|$  were calculated using the phases generated from this interim model. ADP was then fitted to density, followed by stepwise addition of some 150 water molecules. PROLSQ refinement of this intermediate model brought the *R* factor down to 0.19. At this stage, the difference map showed clear density for the phosphorylated form of phosphonate **2**. After the intermediate was fitted into the density, refinement was finalized with the addition of more water molecules to the model, which eventually contained ADP, the phosphorylated phosphonate, 263 water molecules, and three Mg<sup>2+</sup> ions. (The WT/1 model contained only two Mg<sup>2+</sup> ions; here, the third Mg<sup>2+</sup> ion better accounts for density at water position 401 in WT/1.) The WT/2 model resulted in a final *R* factor of 0.155

Table 2: Crystallographic Refinement Results

	WT/2	Y216F/1	WT/1 <sup>a</sup>
resolution (Å)	15–2.2	15–1.9	15–2.3
no. of reflections used [ <i>F</i> > 3 $\sigma$ ( <i>F</i> )]	7591	12800	9776
<i>R</i> factor (%)	15.6	15.8	17.2
<i>R</i> <sub>free</sub> factor <sup>b</sup> (%)	20.4	23.4	17.4
mean <i>B</i> factor (Å <sup>2</sup> )			
protein	9.0	12.9	11.6
inhibitor	5.7	6.5	10.5
water	23.3	22.0	27.1
all atoms	10.3	13.6	13.2
rms deviations from ideality (protein)			
bond lengths (Å)	0.008	0.012	0.013
bond angles (deg)	1.1	1.6	1.7
rms deviations from ideality (inhibitor)			
bond lengths (Å)	0.015	0.034	0.008
bond angles (deg)	1.4	2.2	2.0

<sup>a</sup> From Fan et al. (1994). <sup>b</sup> Calculated with 10% of the reflections selected with X-PLOR.

for data with *F* > 3 $\sigma$ (*F*) from 15 to 2.2 Å. The free *R* factor for this model, evaluated with 10% of the data selected with X-PLOR (Brunger, 1990, 1992), was 0.204. Refinement results for WT/2 are compared in Table 2 with those published for the WT/1 complex (Fan et al., 1994).

**Refinement of the Y216F/1 Complex.** The structure of the Y216F mutant of *E. coli* DD-ligase complexed with **1** was solved by the molecular replacement method using a search model of 305 residues of the WT/1 complex with the exclusion of all atoms of residue Tyr216. The rotation search, PC refinement, and translation search were carried out with X-PLOR (Brunger, 1990). With 3 $\sigma$  data from 15 to 4 Å, the search produced one peak of 19 standard deviations above the background. The crystallographic *R* factor for the molecular replacement solution was 0.32 for the 2342 reflections from 15 to 4 Å. This initial model was refined using X-PLOR, in which the initial temperature for the cooling procedure varied from 3000 to 500 K. When the standard *R* factor for the refinement of this 305-residue model reached 0.25, difference maps with coefficients  $|F_{o,complex}| - |F_{c,protein}|$  showed density of a phenylalanine at position 216. After Phe216, ADP, and phosphorylated phosphinate **1** were fitted into the density, the standard *R* factor reached 0.21. The refinement was completed with stepwise addition of two Mg<sup>2+</sup> ions and 250 water molecules to the model. Crystallographic and free *R* factors for 3 $\sigma$  data from 15 to 1.9 Å resolution are 0.158 and 0.234, respectively (Table 2).

For both refinements, plots of the dependence of *R* factor on resolution (Luzzati, 1952) show that the estimated error in coordinates is about 0.2 Å. Non-glycine outliers in the Ramachandran plot are residues Thr2 and Ala159 in WT/2 and Asp3 and Asp128 in the mutant. In each structure the  $\alpha$ LH region of the plot contains Ser150 and Ser151, important residues in a small loop near the ligand binding sites (see below). *cis*-Prolines occur at positions 140, 186, and 240.

**Common Features of the Complexes.** Electron density maps (Figure 1) clearly show that in each complex the  $\gamma$ -phosphate of ATP has been transferred to the inhibitor. Table 3 lists dihedral angles in the phosphoryl intermediates and compares them with those seen earlier in WT/1 (Fan et al., 1994).

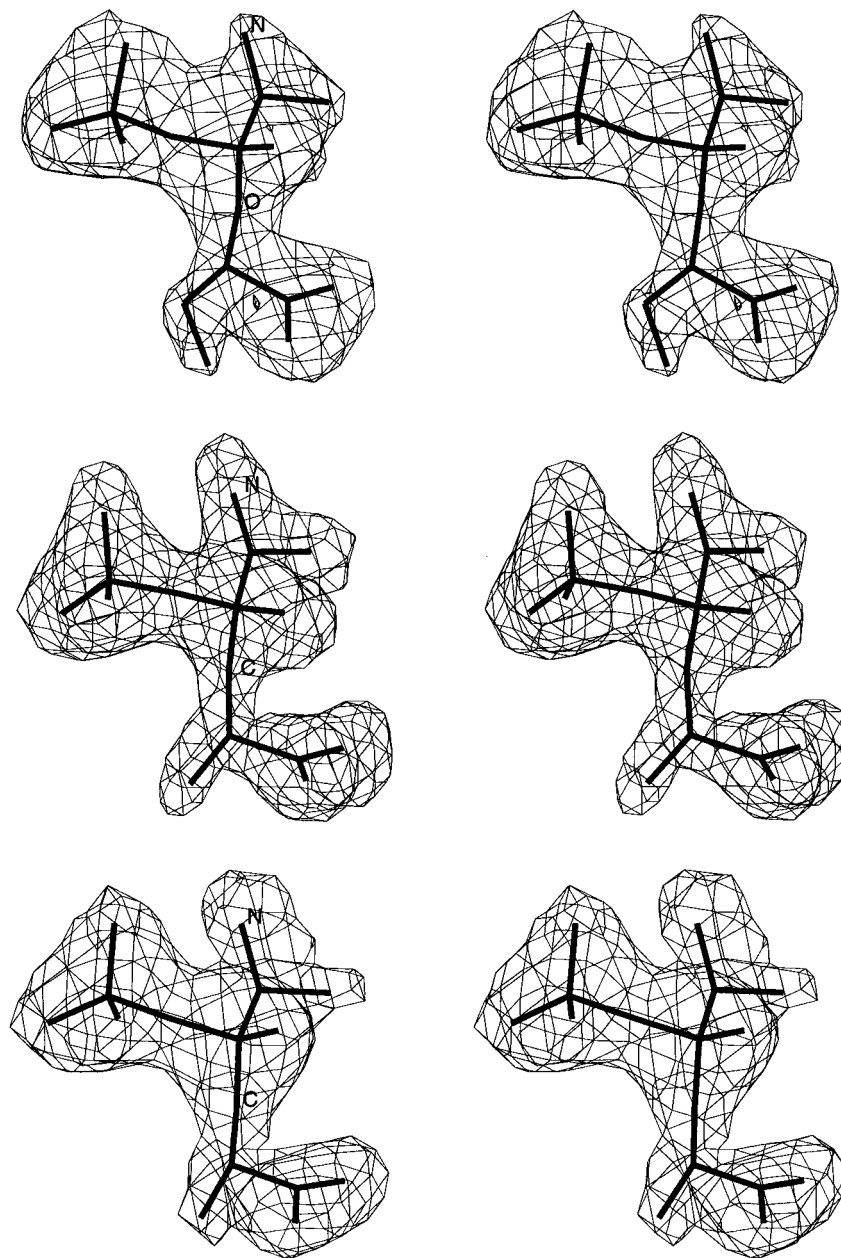


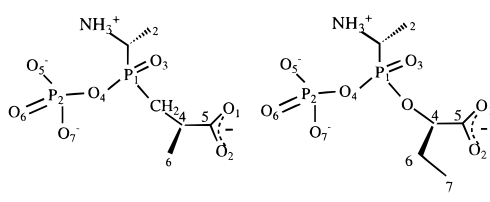
FIGURE 1: Stereoview of the difference electron density of phosphorylated inhibitors (a, top) phosphonate **2** in WT/2, (b, middle) phosphinate **1** in the mutant complex Y216F/1, and (c, bottom) phosphinate **1** in the wild-type complex WT/1 (Fan et al., 1994). Coefficients used were  $F_o - F_c$ , and the inhibitors were omitted from the phase calculation. In each map the contour level is  $3.5\sigma$ . Produced by CHAIN (Sack, 1988).

The 306-residue DD-ligase consists of three  $\alpha+\beta$  domains with a folding motif (Figure 2) common to other ADP-forming C–N bond ligases such as glutathione synthetase (Fan et al., 1995; Hibi et al., 1996; Hiratake et al., 1994), succinyl-CoA synthetase (Murzin, 1996), and biotin carboxylase (Artymiuk et al., 1996). The ATP binding site is between the  $\beta$ -sheets of the central and C-terminal domains, and the inhibitor site is between the central and N-terminal domains. The tight binding of both ligands is reflected in their mean *B* factors being less than that of the polypeptide (Table 2). Figure 3 shows how deeply the ligands are buried in the complex. Only 2% of the ligands' surface is accessible to a probe of 1.4 Å radius. Three loops (13–16, 147–152, and 205–221) cover the ligand binding sites (Figure 4). The loops are connected by a hydrogen-bonded triad Glu15–Ser150–Tyr216. To allow entry and exit of ligands, the

interloop hydrogen bonds possibly break and re-form during each catalytic cycle. *B* factors of these loops and comparison of loop positions in the three complexes are given in Tables 4 and 5, respectively.

**Ligand/Enzyme Interactions.** Distances between the transition state intermediates and groups in the binding site are given in Table 6. An important electrostatic bond in all complexes (distance A1) exists between the  $\alpha$ -ammonium group of the N-terminal D-alanine and the carboxylic acid group of the Glu15 side chain (Figure 5). Ser281 and the backbone amide group of Leu282 bind the C-terminal carboxylic acid group. The oxygen atom of the terminal phosphoryl bond forms two weak hydrogen bonds with the oxyanion pocket of the ligase, formed with the backbone NH of Gly276 and an amino group of Arg255 (distances E1 and E2).

Table 3: Selected Dihedral Angles (deg) in the Three Intermediates

			
	WT/2	Y216F/1	WT/1
N-C1-P1-O4	-37	-28	-30
N-C1-P1-X	-152	-153	-156
C2-C1-P1-X	70	71	73
C1-P1-O4-P2	-41	-61	-47
C1-P1-X-C4	-174	-165	-167
O3-P1-O4-P2	-160	-179	-160
P1-X-C4-C5	104	80	85
P1-X-C4-C6	-139	-153	-153
P1-O4-P2-O5	76	99	94
P1-O4-P2-O6	-36	-13	-18
X-C4-C5-O1	18	38	37
X-C4-C6-C7	-121		
C6-C4-C5-O1	-98	-89	-88
C7-C6-C4-C5	-4		

Interactions of ADP with the ligase (Table 7) include electrostatic links from the  $\alpha$ - and  $\beta$ -phosphate groups to

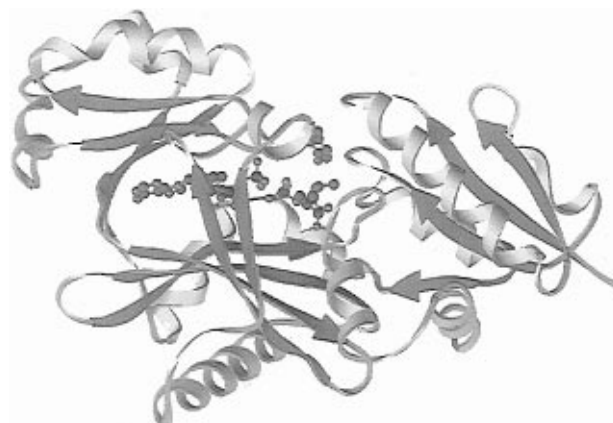


FIGURE 2: View of the DD-ligase with ADP and the phosphorylated inhibitor. The three  $\alpha+\beta$  domains are shown with the N-terminal domain at the right. Tyr216 is seen on the large 205–221 loop. Figure produced with RIBBONS (Carson, 1987).

Lys97, Lys144, and Lys215. Strong hydrogen bonding of the ribose ring with Glu187 and hydrophobic interactions of the adenine ring with W182, F209, and M259 aid the positioning of the nucleotide. In all three complexes the conformation of the ADP is *anti* gauche ( $X = 31\text{--}41^\circ$ , with a 3'-endo ribose ring pucker.

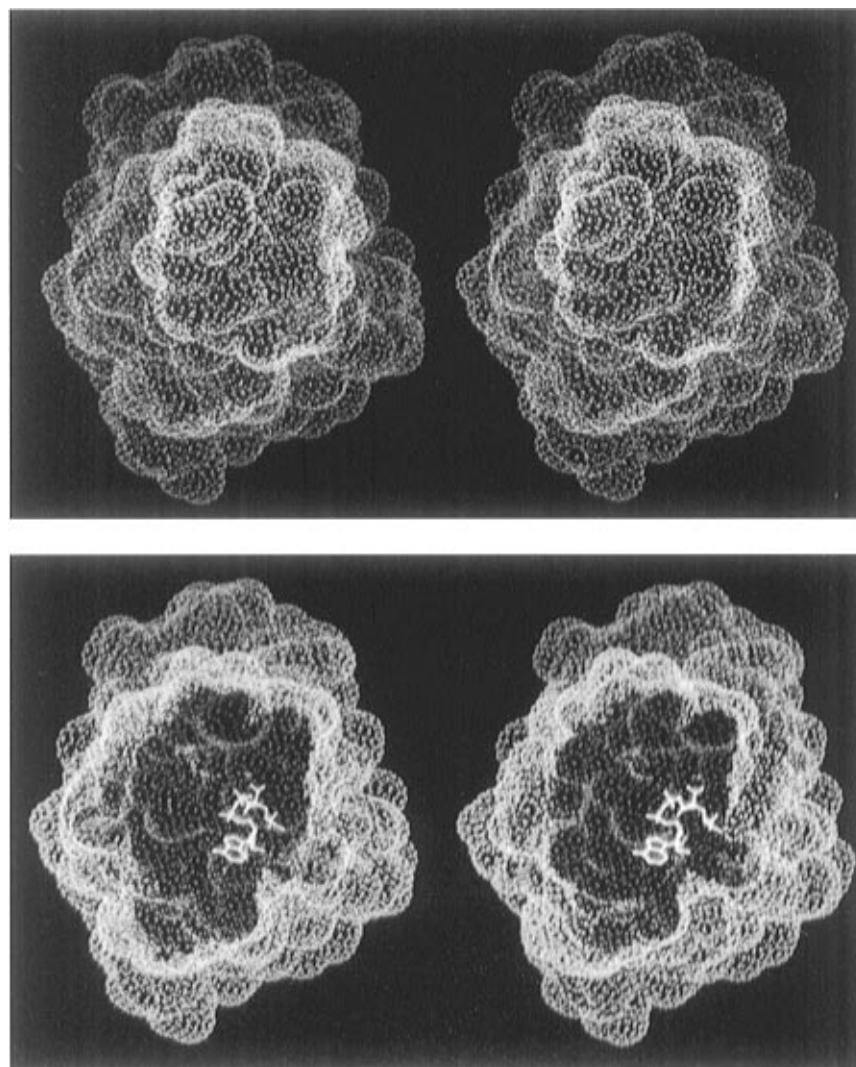


FIGURE 3: (a, top) van der Waals surface of the WT/2 complex, viewed from the left side of Figure 2. (b, bottom) A cut through the complex demonstrating the deep burial of ADP and phosphonate 2. The three loops discussed in the text cover the right side.



FIGURE 4: (a, top) Stereoview of the WT/2 complex showing the three loops discussed in the text: 13–16 (red), 147–152 (green), and 205–221 (blue). Drawn by MOLSCRIPT (Kraulis, 1991). (b, bottom) Overlay of three complexes (WT is dashed) showing the three loops near the ligands. The hydrogen-bonded triad Glu15–Ser150–Tyr216 is shown in the WT complexes. Plotted with FRODO (Jones, 1985).

Table 4: Average *B* Factors ( $\text{\AA}^2$ ) of Loops near Binding Site

	WT/2	Y216F/1	WT/1
loop 13–16	7.2	8.3	7.9
loop 147–152	5.8	10.1	4.5
loop 205–221	9.2	13.3	11.6
all protein	9.0	12.9	11.6

Table 5: Atomic Deviations (rms,  $\text{\AA}$ ) after Pairwise Superpositions<sup>a</sup>

	WT/1–WT/2	WT/1–Y216F/1	WT/2–Y216F/1
loop 13–16	0.32	0.26	0.35
loop 147–152	0.36	0.45	0.60
loop 205–221	0.39	0.82	0.85
intermediate	0.32	0.26	0.33
ADP	0.34	0.73	0.72
C $\alpha$ atoms	0.30	0.42	0.50
all protein	0.47	0.80	0.85

<sup>a</sup> All atoms in complex used in superposition.

## DISCUSSION

**Comparison of the Two WT Complexes.** Differences in size and character of inhibitors **1** and **2** produce little

crystallographic difference in their complexes with the wild-type ligase; the rms deviation between equivalent  $\alpha$ -carbon atoms is only 0.3  $\text{\AA}$  (Table 5). The three loops over the ADP and inhibitor binding sites (Figure 4) do not differ significantly in position from one wild-type complex to another, and all loops show about the same rms differences (0.3–0.4  $\text{\AA}$ , all atoms). These differences are somewhat smaller than for all atoms throughout the protein (0.5  $\text{\AA}$ ), possibly because of interloop hydrogen bonding (Glu15–Ser150–Tyr216) and the attractive interactions between the loops and the intermediate. In like manner, when the mobility of the loops is estimated via their average *B* factors, two of the three loops show less mobility than the whole molecule (Table 4).

**Comparison of WT and Y216F Mutant.** With the loss of the hydrogen bond from Tyr216 to Ser150, the loops in Y216F/1 are expected to exhibit larger *B* factors relative to those in the two WT complexes (Table 4). Differences in atom positions are generally larger when the mutant complex is compared with either WT complex than when one WT complex is compared with the other (Table 5). Especially

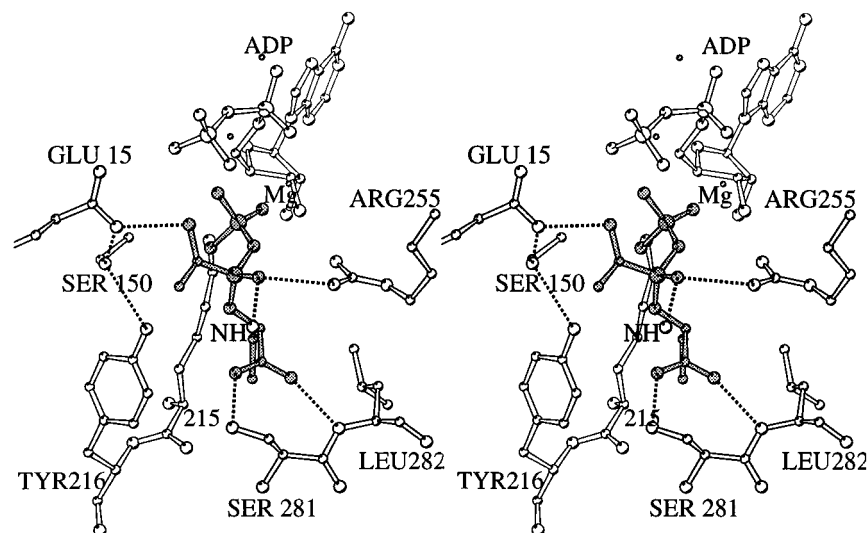


FIGURE 5: Phosphorylated inhibitor in the binding site of the WT/2 complex. Hydrogen bonds are dashed.  $\text{Mg}^{2+}$  ions bridging ADP and the inhibitor are shown. The NH group of Gly276 helps to form an oxyanion pocket with Arg255. Drawn by MOLSCRIPT (Kraulis, 1991).

Table 6: Distances (Å) between Intermediates and Binding Site Residues

	WT/2	Y216F/1	WT/1
distance (X = O, Y = $\text{C}_2\text{H}_5$ ) (X = $\text{CH}_2$ , Y = $\text{CH}_3$ ) (X = $\text{CH}_2$ , Y = $\text{CH}_3$ )			
A1	2.7	3.0	2.8
A2	2.4	2.8	2.6
B	3.3	2.8	3.4
C1	2.9	3.2	2.5
C2	2.8	2.9	3.1
D1	3.2	3.0	2.4
D2	2.5	2.6	2.6
E1	3.0	3.0	3.2
E2	2.9	3.0	3.1
F1	3.0	2.5	2.4
F2	2.6	3.1	2.8
G	2.2	2.6	2.3
J1	3.3		3.5
J2	2.9		2.8
K1	2.5	3.0	2.8
K2	3.2	3.0	2.8
L1	2.4	2.0	2.3
L2	2.2	2.0	2.3
M1	2.4	2.2	2.6
M2	2.0	2.0	1.9

in these cases, the 205–221 loop is displaced more than the two smaller loops.

**Binding of Phosphinate and Phosphonate Intermediates to WT Ligase.** The larger ethyl substituent on the phosphonate **2** is easily accommodated without significant distortion of the binding site (Table 5), in agreement with the broad specificity for hydrophobic side chains at this site (Parsons

Table 7: Distances (Å) between ADP and Binding Site Residues

distance	WT/2	Y216F/1	WT/1
A	2.5	2.8	3.1
B1	3.5	2.8	3.1
B2	3.5	3.2	3.1
C	2.5	2.9	3.0
D	3.2	3.0	3.0
E	2.6	2.8	2.8
F	3.2	3.0	2.8
G	2.1	2.4	2.4
J	2.4	2.8	2.5
K	3.0	3.2	3.1
L	2.8	3.3	3.3
M	3.3	2.7	2.6

et al., 1988). The presence of a displaceable water molecule at the bottom of the binding site (Figure 5) allows the enzyme to accept side chains larger than methyl on the C-terminal  $\alpha$ -carbon atom. Accordingly, inhibition constants for leucyl and phenyl analogs in the ddIA, ddIB, and VanA ligases are lower or equal to those for methyl and ethyl analogs (Ellsworth et al., 1996).

Atoms in phosphorylated **2** are within 0.3 Å (rms) of corresponding atoms in **1**, comparable to the fit of the two sets of  $\alpha$ -carbon atoms in the WT polypeptide. All hydrogen-bonding and electrostatic interactions with the binding site are generally equivalent for the two intermediates (Table 6), with strong bonding to amino and carboxy termini and to the phosphoryl group via  $\text{Mg}^{2+}$  cations and Lys215. The

Table 8: Relative Reversible Inhibition Constants  $K_i$  (nM)

analog	WT	Y216F	VanA
D-Ala[PO <sub>2</sub> -CH <sub>2</sub> ]D-Ala <b>1</b>	33, <sup>a</sup> 3 <sup>b</sup>	7800, <sup>c</sup> 1900 <sup>b</sup>	4100 <sup>b</sup>
D-Ala[PO <sub>2</sub> -O]D-HBUT <b>2</b>	13 <sup>b</sup>	2700, <sup>c</sup> 650 <sup>b</sup>	6800 <sup>b</sup>

<sup>a</sup> From Shi and Walsh (1995). <sup>b</sup> From Ellsworth et al. (1996). <sup>c</sup> From Park et al. (1996).

hydrogen bonds to the terminal P—O bond in the oxyanion hole are rather weak in each complex ( $>2.9$  Å). These bonds would presumably be stronger during formation of the Michaelis complex, because in the unphosphorylated inhibitor the oxyanion state of the terminal oxygen atom is more prevalent.

Of the three loops closing over the phosphorylated intermediate (Figure 4), the largest loop has the highest average  $B$  factor. This loop has a slightly lower  $B$  factor in WT/2, as does the bound intermediate **2**, perhaps because of increased hydrophobic binding to the ethyl group.

The relative values of the  $B$  factors for intermediates **1** and **2** in the WT ligase (10.5 and 5.7 Å<sup>2</sup>) correlate well with the length of most hydrogen bonds and electrostatic bonds (Table 6). It is not possible to correlate this information with  $K_i$  values for reversible inhibition (Table 8) because of the wide range of published values of the  $K_i$ . The 4-fold tighter binding of the phosphinate shown by one study (Ellsworth et al., 1996) might arise from the weak CH $\cdots$ O hydrogen bond from the methylene group to the hydroxyl of Tyr216. This argument is weakened by the fact that the homologous ddlA ligase, which contains an equivalent tyrosine, exhibits much tighter binding (40-fold) for the phosphinate. The VanA ligase, apparently without a tyrosine in this loop, shows little discrimination and very weak binding for both inhibitors. By a similar analysis of binding constants, Ellsworth et al. (1996) have argued that the relative binding of phosphinate and phosphonate inhibitors to this and other enzymes has little dependence on active site interactions, depending instead on relative differences in inhibitor solvation. This hypothesis agrees with the fact that we observe in the crystal structures of these three complexes no significant differences in the conformation of the binding site.

**Binding of the Phosphinate Intermediate to the Y216F Mutant.** Hydrogen bonding between the phosphorylated intermediate **1** and the Y216F mutant is generally weaker than that between the intermediate and the wild-type ligase (A1, C1, F2, K1 in Table 5). Increased mobility of the three loops in Y216F relative to WT (Table 4) would account for some increase in certain hydrogen bond lengths. For example, Glu15 on the smaller loop and its attached water molecule form weaker bonds (A1 and C1) to the  $\alpha$ -amino group of the intermediate in Y216F. Lys215 in the larger loop binds the intermediate's phosphoryl group (K1) more weakly in Y216F than in WT. Perhaps as a result of these factors, the  $K_i$  for inhibition by **1** of the Y216F mutant is several orders of magnitude greater than for the wild-type ligase (Table 8).

For inhibitors **1** and **2** the  $K_i$  differs by less than an order of magnitude for any given ligase, but the  $K_i$  differs by  $10^2$ – $10^3$  when comparing the wild-type ligase to the Y216F mutant or to VanA (Table 8). The modification of the tyrosine in the large loop, or its assumed absence in VanA, leads to high  $K_i$  values, presumably because loss of the

interloop hydrogen bond produces increased mobility and results in weaker interaction with these inhibitors.

**Relation to VanA and Other Depsipeptide Ligases.** The altered DD-ligase (VanA) produced by vancomycin-resistant enterococci has both depsipeptide- and peptide-forming activities, with optimum D-Ala-D-hydroxybutyrate activity near pH 6 and D-Ala-D-Ala activity near pH 9 (Park et al., 1996), as does the Y216F ddlB mutant examined here. The crystal structure of VanA is not yet known, but it has been proposed that the 30% identity in primary sequence between VanA and the wild-type ddlB DD-ligase extends to the level of tertiary structure (Fan et al., 1994). Important residues assumed to be common to the inhibitor binding site of the two ligases are Glu15, Ser150, Ser281, and Arg255 (Figure 5). Because sequence alignment in the important 205–220 loop remains unclear for VanA, the identity of the “gate” residue at 216 near the second substrate is not certain. An examination of sequences in the 205–220 loop of eight other DD-ligases from both vancomycin-sensitive and vancomycin-resistant bacteria (Park et al., 1996) shows a strong correlation of tyrosine at the position equivalent to 216 in vancomycin-sensitive organisms and phenylalanine in vancomycin-resistant organisms. This Y/F switch correlates with peptide/depsipeptide ligase activity in this particular set of sequences (Park et al., 1996). However, the enterococcal VanA ligase contains neither tyrosine nor phenylalanine near this position of the loop.

Interestingly, the Y216F ddlB mutant, described above, has a low level of depsipeptide-forming activity, about 5–10% of that of VanA. This depsipeptide activity is significantly higher than that shown by the wild-type ligase and, moreover, has a pH profile more similar to that of VanA (Park et al., 1996). Thus, it is likely that the *E. coli* Y216F ddlB ligase will be a good model structurally and mechanistically for both soil organisms (lactobacilli, leuconostoc) and opportunistic pathogens (enterococci) that possess vancomycin-resistant phenotypes that derive from the ability to incorporate D-Ala-D-lactate in place of D-Ala-D-Ala into peptidoglycan termini. It is not yet obvious how a Y/F switch permits selective activation of D-lactate in competition with D-alanine in the active site of many ligases.

## ACKNOWLEDGMENT

We thank Bruce Ellsworth and Prof. Paul Bartlett, University of California, Berkeley, for providing the phosphinate and phosphonate analogs. They and Yian Shi, Harvard, contributed to discussions of ligand kinetics. Paul Moews provided computational assistance.

## REFERENCES

- Arthur, M., & Courvalin, P. (1993) *Antimicrob. Agents Chemother.* 37, 1563–1571.
- Artymiuk, P. J., Poirrette, A. R., Rice, D. W., & Willett, P. (1996) *Nat. Struct. Biol.* 3, 128–132.
- Brunger, A. T. (1990) *X-PLOR Manual, Version 2.1*, Yale University, New Haven, CT.
- Brunger, A. T. (1992) *Nature* 355, 472–475.
- Carson, M. (1987) *J. Mol. Graphics* 5, 103–106.
- Chakravarty, P. K., Greenlee, W. J., Parsons, W. H., Patchett, A. A., Combs, P., Roth, A., Busch, R. D., & Mellin, T. N. (1989) *J. Med. Chem.* 32, 1886–1890.
- Duncan, K., & Walsh, C. T. (1988) *Biochemistry* 27, 3709–3714.
- Duncan, K., Faraci, W. S., Matteson, D. S., & Walsh, C. T. (1989) *Biochemistry* 28, 3541–3549.

- Dutka-Malen, S., Molinas, C., Arthur, M., & Courvalin, P. (1990) *Mol. Gen. Genet.* 224, 364–372.
- Ellsworth, B. A., Tom, N. J., & Bartlett, P. A. (1996) *Chem. Biol.* 3, 37–44.
- Fan, C., Moews, P. C., Walsh, C. T., & Knox, J. R. (1994) *Science* 266, 439–443.
- Fan, C., Moews, P. C., Shi, Y., Walsh, C. T., & Knox, J. R. (1995) *Proc. Natl. Acad. Sci. U.S.A.* 92, 1172–1176.
- Hibi, T., Nishioka, T., Kato, H., Tanizawa, K., Fukui, T., Katsube, T., & Uda, J. (1996) *Nat. Struct. Biol.* 3, 16–18.
- Hiratake, J., Kato, H., & Oda, J. (1994) *J. Am. Chem. Soc.* 116, 12059–12060.
- Howard, A. J., Gilliland, G. L., Finzel, B. C., Poulos, T. L., Ohlendorf, D. H., & Salemme, F. R. (1987) *J. Appl. Crystallogr.* 20, 383–387.
- Jones, T. A. (1985) *Methods Enzymol.* 115, 157–170.
- Knox, J. R. (1995) *Antimicrob. Agents Chemother.* 39, 2593–2601.
- Konnert, J. H., & Hendrickson, W. A. (1980) *Acta Crystallogr., Sect. A* 36, 344–349.
- Kraulis, P. (1991) *J. Appl. Crystallogr.* 24, 946–950.
- Leclercq, R., Derlot, E., Duval, J., & Courvalin, P. (1988) *N. Engl. J. Med.* 319, 157–161.
- Luzzati, V. (1952) *Acta Crystallogr.* 5, 802–810.
- McDermott, A. E., Creuzet, F., Griffin, R. G., Zawadzke, L. E., Ye, Q.-Z., & Walsh, C. T. (1990) *Biochemistry* 29, 5767–5775.
- Mullins, L. S., Zawadzke, L. E., Walsh, C. T., & Rauschel, F. M. (1990) *J. Biol. Chem.* 265, 8993–8998.
- Murzin, A. G. (1996) *Curr. Opin. Struct. Biol.* 6, 386–394.
- Neuhaus, F. C., & Hammes, W. P. (1981) *Pharmacol. Ther.* 14, 265–319.
- Neuhaus, F. C., & Lynch, J. L. (1964) *Biochemistry* 3, 477–480.
- Park, I.-S., Lin, C.-H., & Walsh, C. T. (1996) *Biochemistry* 35, 10464–10471.
- Parsons, W. H., Patchett, A. A., Bull, H. G., Schoen, W. R., Taub, D., Davidson, J., Combs, P., Springer, J. P., Gadebusch, H., Weissberger, B., Valiant, M. E., Mellin, T. N., & Busch, R. D. (1988) *J. Med. Chem.* 31, 1772–1778.
- Sack, J. S. (1988) *J. Mol. Graphics* 6, 224–225.
- Shi, Y., & Walsh, C. T. (1995) *Biochemistry* 34, 2768–2776.
- Spratt, B. G. (1994) *Science* 264, 388–393.
- Walsh, C. T. (1993) *Science* 261, 308–309.
- Zawadzke, L. E., Bugg, T. D. H., & Walsh, C. T. (1991) *Biochemistry* 30, 1673–1682.

BI962431T